

Synthesis, Structural Analysis and Thermal Behavior of New 1,2,4-Triazole Derivative and Its Transition Metal Complexes

Ali Talib Bader^{1*}, Nada Ahmed Rasheed Al-qasii², Ahmed Hassen Shntaif¹, Maryam El Marouani³, Mohammed Idaan Hassan AL Majidi^{1,4}, László Trif⁵, and Mohammed Boulhaoua⁴

¹Department of Chemistry, College of Sciences for Woman, University of Babylon, Hilla, Iraq

²Department of Chemistry, College of Science, University of Baghdad, Baghdad, Iraq

³Department of Chemistry, College of Sciences, University of Hafr Al Batin, Hafr Al Batin, Kingdom of Saudi Arabia

⁴Institute of Chemistry, ELTE Eötvös Loránd University, Pázmány Péter sétány 1/A, H-1117, Budapest, Hungary

⁵Institute of Materials and Environmental Chemistry, Research Centre for Natural Sciences, Budapest, Hungary

* Corresponding author:

tel: +964-7710783571

email: wsc.ali.taleb@uobabylon.edu.iq

Received: September 3, 2021

Accepted: November 3, 2021

DOI: 10.22146/ijc.68859

Abstract: Cobalt(II), nickel(II), and copper(II) complexes containing bidentate ligands (5-(4-nitrophenyl)-4-((4-phenoxybenzylidene)amino)-4H-1,2,4-triazole-3-thiol) could be synthesized by the condensation reaction between 1,2,4-triazole derivative and p-phenoxy benzaldehyde. The ligand and its complexes were characterized by various spectroscopic techniques such as FTIR, UV-visible, ¹H and ¹³C-NMR, element analysis, molar conductance, and magnetic susceptibility test. The new ligand was exploited as a ligand to coordinate with Co(II), Ni(II), and Cu(II) by a molar ratio of 1:2 (metal:ligand). The prepared complexes (C₁, C₂, and C₃) were exposed to thermo-gravimetric analysis (TGA/DTG) under an inert atmosphere to investigate their thermal stability. The ligand (L) degradation was also investigated as a reference. The results indicated that the complexes proposed structures had an octahedral geometry.

Keywords: 1,2,4-triazole; Schiff base; thermal analysis; metal complexes

■ INTRODUCTION

Heterocyclic compounds are organic molecules that contain a minimum of two different atom types in the ring [1]. Heterocyclic compounds with different donor atoms, like S, N, or O, tend to form metal chelates or coordination compounds utilized as active antibacterial agents [2]. 1,2,4-triazole is one of the most important aromatic heterocyclic nitrogen-rich molecules [3-4]. There is increasing attention to the triazole substructure's potential application as urease and lipase enzyme inhibitors [5]. Linking the triazole moiety to a reasonably selected and different biologically active agent fragment would form new complexes that might have better biological activity because of the synergistic effects [6-7].

Furthermore, these compounds have multiple sites for metal atoms to coordinate with, forming more stable transition metal complexes that are bioactive triazole-

based. Recently, significant effort has been devoted to studying the thermal degradation characteristics under inert and oxidative atmospheres. In this work, we determined the first synthesis and characterization of a new Schiff base triazole derivative and its cobalt(II), nickel(II), and copper(II) complexes. Common spectroscopic techniques such as ¹H-NMR, ¹³C-NMR, FTIR, UV-Vis, elemental analysis, and thermal analysis were used to characterize the synthesized compounds. We have examined the thermal degradation profile of the prepared complexes to highlight their energy potential and the far-reaching possibilities of their use.

■ EXPERIMENTAL SECTION

Materials

The 4-nitro benzoic acid, absolute ethanol, hydrazine hydrate 80%, acetic acid, carbon disulfide,

potassium hydroxide, and 4-phenoxy benzaldehyde were supplied by Sigma-Aldrich (Germany), and the metal salt $\text{CoCl}_2 \cdot 6\text{H}_2\text{O}$, $\text{NiCl}_2 \cdot 6\text{H}_2\text{O}$, and $\text{CuCl}_2 \cdot 6\text{H}_2\text{O}$ were supplied by Fluka (Germany). All chemicals were used without further purification.

Instrumentation

The Nuclear magnetic resonance (NMR) measurements of the synthesized compounds were performed at 500 MHz in DMSO-d_6 at 25 °C on Bruker DRX-500 spectrometer using the deuterium signal of the solvent as the lock and tetramethylsilane (TMS) as the internal standard. Varian 2000 (Scimitar Series) FTIR spectrometer with MCT (mercury-cadmium-telluride) detector and single reflection diamond ATR unit (Varian Inc., US) (Specac Ltd, UK) was used to record infrared (IR) spectra. For a single spectrum, 32 individual scans were averaged at a resolution of 4 cm^{-1} , and the instrument's data acquisition software (ResPro 4.0) was used to ATR-correct all the spectra. A PerkinElmer UV/Vis Lambda 35 spectrometer was used to conduct the spectrophotometric measurements by applying acetonitrile as a solvent and a slit width of 1 nm.

Procedure

Synthesizes of ethyl 4-nitrobenzoate

Dropwise additions of H_2SO_4 (3 mL) to a mixture of 5 g (0.025 mol) of 4-nitrobenzoic acid in 50 mL ethanol were heated under reflux for 6 h. The precipitate formed after cooling, and the excess ethanol was evaporated. The solid product was washed with a sodium bicarbonate solution, filtered, rinsed with cold water, dried, and recrystallized from ethanol to yield, as shown in Scheme 1.

Synthesizes of 4-nitrobenzohydrazide

Hydrazine hydrate (80%, 20 mL) was added to a solution of ethyl 4-nitrobenzoate by dissolving (5 g, 0.027 mol) in 50 mL of absolute ethanol, and then the mixture was heated under reflux for 8 h. Finally, the mixture was allowed to cool, and a solid product was filtered, washed with cold water, dried, and recrystallized from ethanol to produce 4-nitrobenzohydrazide, as shown in Scheme 1.

Synthesized of potassium 2-(4-nitrobenzoyl)hydrazine-1-carbodithioate

The 4-nitrobenzohydrazide (4 g, 0.022 mol) was treated at 0 °C with stirring in a solution of 2.5 g (0.044 mol) potassium hydroxide in 40 mL ethanol. Dropwise additions of 7 mL (0.2 mol) carbon disulfide were made to the reaction mixture, agitated overnight at room temperature. The reaction was then cooled with 200 mL diethyl ether, which was agitated for 10 min. The solid result was then filtered, washed with cold ethanol, and dried to yield potassium 2-(4-nitrobenzoyl)hydrazine-1-carbodithioate, as shown in Scheme 1.

Synthesis of 4-amino-5-(4-nitrophenyl)-4H-1,2,4-triazole-3-thiol

The synthesis used a reported procedure in the literatures [8-9]. Potassium 2-(4-nitrobenzoyl)hydrazine-1-carbodithioate (3.5 g, 0.011 mol) was heated under reflux for 6 h in excess of hydrazine hydrate (approximately 30 mL). The color of the lead acetate sheet changed from black to white to release hydrogen sulfide gas by changing the color of the mixture from black-green to light yellow. The chilled mixture was put into 30 mL of ice water and acidified with concentrated hydrochloric acid (pH 2-3). To get 4-amino-5-(4-nitrophenyl)-4H-1,2,4-triazole-3-thiol, the precipitate was filtered, rinsed with cold water, dried, and recrystallized from ethanol.

Synthesis of Schiff base (ligand L)

A hot solution of 4-amino-5-(4-nitrophenyl)-4H-1,2,4-triazole-3-thiol (0.237 g, 1 mmol) in 15 mL of EtOH was added dropwise to a solution of *p*-phenoxybenzaldehyde (0.198 g, 0.001 mol) in the presence of three drops of glacial acetic acid (AcOH). The reaction mixture was refluxed for 4 h. The resulting yellow compound was filtered and then dried in air to yield the required Schiff base ligand (L) as a yellow solid (yield: 78%, MP: 270-272 °C) (Scheme 1).

Synthesis of metal ions complexes

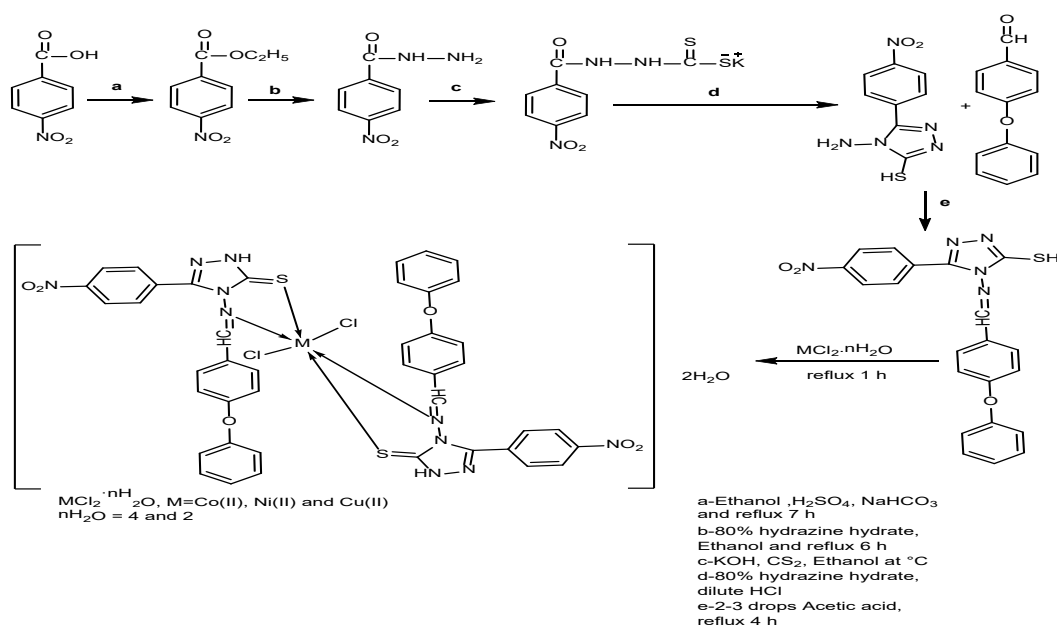
The complexes (C_1 , C_2 , C_3) were synthesized as shown in Scheme 1 by adding the hot ethanolic solution of the metal ions ($\text{CoCl}_2 \cdot 6\text{H}_2\text{O}$, $\text{NiCl}_2 \cdot 6\text{H}_2\text{O}$, and $\text{CuCl}_2 \cdot 2\text{H}_2\text{O}$) to the hot ligand (L) (0.834 g, 2 mmol)

ethanolic solution in 1:2 (metal: ligand) molar ratio. The reaction mixture was refluxed for 1 h, and colored precipitates were formed. Then, the obtained complexes were filtered and recrystallized from ethanol. Table 1 shows the number of metal salts in the complexes [10].

RESULTS AND DISCUSSION

Table 2 shows the results of metal content determination by atomic absorption, chloride content,

CHNS elemental analysis, and the physical features of the ligand and its metal complexes. The suggestion of the molecular formula of the studied compounds was made relying on spectral data, atomic absorption analysis, chloride content, CHNS, and conductivity measurements. Table 2 shows the metal complexes' analytical data. The complexes formation was revealed by these data having a 1:2 (ligand:metal ion) ratio, showing that the Schiff base ligand was a chelating agent.



Scheme 1. Synthesis pathway of Schiff base (ligand L) and their metal complex

Table 1. Amount of metal salts in the complexes

Complex symbol	Complexes formal	Metal salts	Weight metal salts (g)
C1	$[Co(L)_2Cl_2] \cdot 2H_2O$	$CoCl_2 \cdot 6H_2O$	0.237
C2	$[Ni(L)_2Cl_2] \cdot 2H_2O$	$NiCl_2 \cdot 6H_2O$	0.237
C3	$[Cu(L)_2Cl_2] \cdot 2H_2O$	$CuCl_2 \cdot 2H_2O$	0.170

Table 2. Physical properties and analytical data for synthesized ligand and its metal ion complexes

Product	Color	Yield	Molar mass (g mol)	Micro elemental analysis found (calc.)				% Metal content found (calc.)	% Chloride content found (calc.)
				% C	% H	% N	% S		
(L)	Yellow	70	417.44	59.90 (60.42)	3.44 (3.62)	3.44 (3.62)	7.20 (7.68)	--	--
C ₁	Brown	65	998.73	51.90 (52.05)	2.60 (2.91)	2.60 (2.91)	6.02 (6.62)	6.12 (6.75)	6.96 (7.32)
C ₂	Green	70	988.73	44.66 (44.87)	3.11 (3.59)	3.11 (3.59)	5.20 (5.70)	7.80 (7.50)	5.97 (6.31)
C ₃	Yellow	70	1033	45.01 (45.68)	2.12 (2.56)	2.12 (2.56)	5.81 (5.44)	6.12 (6.33)	6.42 (7.81)

FTIR Spectrometric Analysis

Compared to the spectrum shown in Fig. 1, the FTIR spectra of the ligand (L) showed various alterations of 4-amino-5-(4-nitrophenyl)-4*H*-1,2,4-triazole-3-thiol. At 3160 cm^{-1} , there was a medium intensity band associated with the $\nu(\text{NH})$ group. The disappearance of a band at 3890 and 3400 cm^{-1} was due to the stretch of $\nu(\text{NH}_2)$ (asymmetry and symmetry). The appearance of a new set of sharp stretching vibration bands at the frequency that is identical to the $\nu(\text{C}=\text{N})$ imine group confirmed the formation of Schiff base at 1568 cm^{-1} , and $\nu(\text{S}-\text{H})$ appeared as a weak band at 2550 cm^{-1} . In all the complexes,

the $(\text{C}=\text{N})$ imine group in the ligand (L) was moved to a lower wavenumber, indicating that the $(\text{C}=\text{N})$ imine group was coordinated with the metal via the N atom. However, in the spectra of prepared micro complexes, the $(\text{C}=\text{S})$ stretching vibration shifted to higher frequencies or appeared as multiple bands with different shapes and reduced intensity. This frequency shift, change in form, and location for the stretching vibrations of the $(\text{C}=\text{N})$ imine and $(\text{C}=\text{S})$ group showed the coordination of metal ion with (N) atom of imine group and (S) atom of thiol group. Table 3 lists the important stretching vibrations of ligands and their complexes [11].

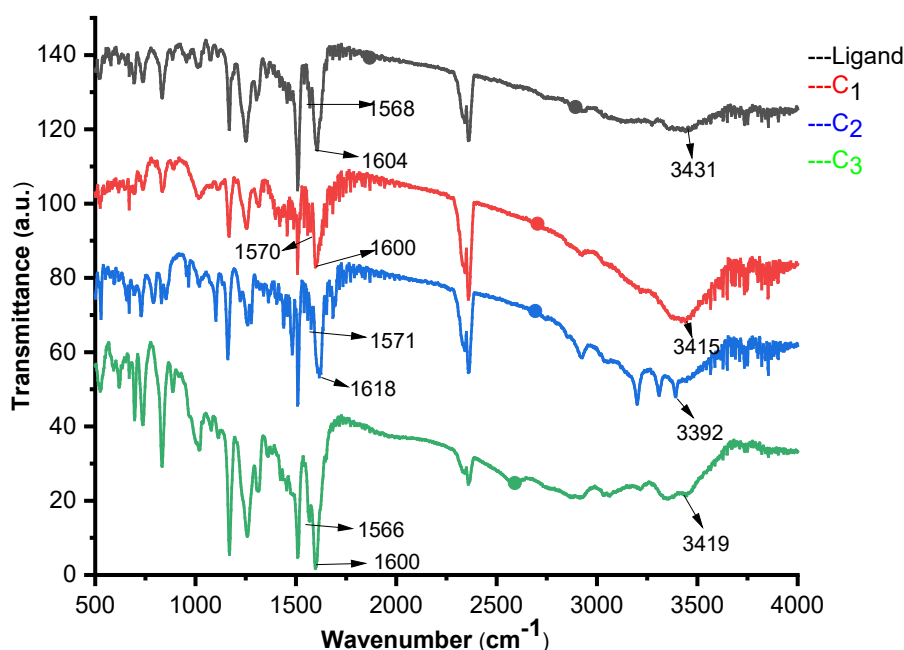


Fig 1. FTIR spectra of the Schiff base (ligand L) and its metal ion complexes (C₁ to C₃)

Table 3. FTIR spectral data of Schiff base (Ligand) and its complexes

Bond	Wavenumber (cm^{-1})			
	Ligand (L)	Complex (C ₁)	Complex (C ₂)	Complex (C ₃)
N-H	3431	3415	3392	3419
C=N (imine)	1568	1571	1577	1566
C=N (triazole)	1604	1600	1618	1598
C=S _{st}	1167	1167	1162	1169
N-O	1510	1510	1510	1510
C-O-C	1249	1253	1276	1257
=C-H (aromatic)	3033	3033	3043	3033
C-H (aromatic)	694-835	698-835	698-831	696-831
C=C (aromatic)	1681	1679	1689	1685

Electronic Spectra, Magnetic Susceptibility and Molar Conductance

In a DMF solution, the UV-visible absorption spectra of ligand L are shown in Fig. 2 and summarized in Table 4. Two bands at 265 nm and 318 nm were assigned to the ($\pi-\pi^*$) transition while a band at 318 nm was

assigned to the ($n-\pi^*$) transition. In the visible region, the electronic spectra of C_1 complex in DMF solvent showed two spin-allowed bands at 435 nm and 622 nm, which could be associated with the transitions of the ${}^4T_{1g} \rightarrow {}^4T_{2g}(f)$ (ν_2) and ${}^4T_{1g} \rightarrow {}^4T_{1g}(p)$ (ν_3), respectively. The C_1 complex was paramagnetic, as indicated by its magnetic

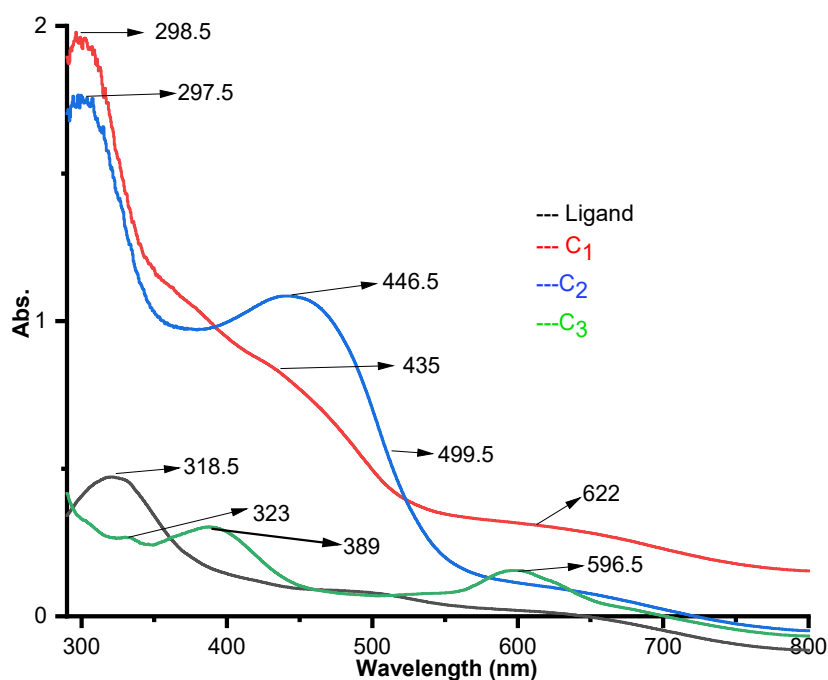


Fig 2. Electronic spectra of the ligand and its metal complexes

Table 4. Magnetic susceptibility, molar conductivity, and electronic spectral data of ligand(L)

Compound	λ_{\max} nm (ν cm^{-1})	Assignment	Molar conductivity $\text{ohm}^{-1} \text{cm}^2 \text{mol}^{-1}$	Magnetic susceptibility (BM) found (calc.)	Suggested geometry
Ligand	265 (37735.84)	($\pi-\pi^*$)	-	-	Octahedral geometry
	318 (31446.54)	($n-\pi^*$)			
C_1	435 (22988.50)	${}^4T_{1g} \rightarrow {}^4T_{2g}(f)$	39.00	3.9 (3.87)	Octahedral geometry
	622 (16077.17)	${}^4T_{1g} \rightarrow {}^4T_{1g}(p)$			
C_2	499.5 (20020.02)	${}^3A_{2g} \rightarrow {}^3T_{1g}(f)$	50.2	3.10 (2.8)	Octahedral geometry
	446 (22421.52)	${}^3A_{2g} \rightarrow {}^3T_{1g}$			
C_3	596.5 (16764.45)	${}^2B_{1g} \rightarrow {}^2B_{2g} + {}^2E_g$	1.63	1.63	Octahedral geometry
	398 (25125.62)	${}^2B_{1g} \rightarrow {}^2A_{1g}$			

susceptibility of 3.9 BM, and the complex had a molar conductivity of $39.00 \text{ ohm}^{-1} \text{ cm}^2 \text{ mol}^{-1}$ indicating that it was non-conductive as indicated in Table 4. In addition to this information, the results of elemental (CHNS) analysis, flame atomic absorption, and FTIR spectrum supported this hypothesis, and implied an octahedral structure for the C_1 complex as shown in Fig. 3 [12]. The C_2 complex's electronic spectra in DMSO solution revealed two spin-allowed bands of 499.5 nm and 446 nm, which corresponded to the ${}^3A_2g \rightarrow {}^3T_1g$ (f) and ${}^3A_2g \rightarrow {}^3T_1g$ (p) transitions, respectively. Around the Ni(II) ion, these bands indicated an octahedral shape. The magnetic moment value for Ni(II) in Table 3 was 3.10 BM, which was within the range of 2.8–3.5 BM for Ni(II) ion with octahedral geometry. The conductivity of this compound referred to its non-ionic performance. Thus, based on the information presented above, as well as those derived from FTIR spectra and flame atomic absorption, an octahedral geometry around the Ni(II) ion can be proposed as shown in Fig. 3 [13-14]. The d^9 ion was characterized by a large distortion from the octahedral symmetry, and the band was asymmetrical. Several transformations have occurred, and these transitions have emerged, which cannot be easily set without ambiguity. The free ion 2D term was expected to split in a crystal field in the same way as the 5D term of the d^4 ion, and a similar interpretation of the spectra was likewise expected. The

spectrum of Cu(II) complex in the DMF solution showed one broadband at 596.5 nm which agreed with ${}^2B_{1g} \rightarrow {}^2B_{2g} + {}^2E_g$ ($\nu_2 + \nu_3$) transition, and shoulder band at 398 nm allocated to ${}^2B_{1g} \rightarrow {}^2A_{1g}$ (ν_1) transitions. The purpose of these bands was to approve extremely warped octahedral geometry with their configuration. At room temperature, the magnetic moment was 1.80 BM. The complex's conductivity in DMF revealed that it was non electrolytic. As shown in Fig. 2 the octahedral geometry around the Cu(II) ion might be inferred from the electronic spectra, FTIR spectroscopy data, and flame atomic absorption Fig. 3 [15].

NMR Studies

1H -NMR of Schiff base (ligand L)

Fig. 4 displays the signal assignments for the 1H -NMR spectrum of Schiff base (ligand L) in DMSO- d_6 . A key singlet 8.51 ppm (1H) was observed corresponding to the Schiff base proton [13]. The chemical shifts of aromatic and triazole ring protons were exhibited at 6.3–8.08 ppm, respectively. The spectrum showed a strong peak of thiol proton singlet at 13.10 ppm (1H) [16-17].

${}^{13}C$ -NMR of Schiff base (ligand L)

The ${}^{13}C$ -NMR spectra of the ligand is depicted in Fig. 5. The presence of the (N=CH) azomethine group in the ligand's spectra, which occurred at 158 ppm, was a distinguishing feature. Aromatic carbons shifted

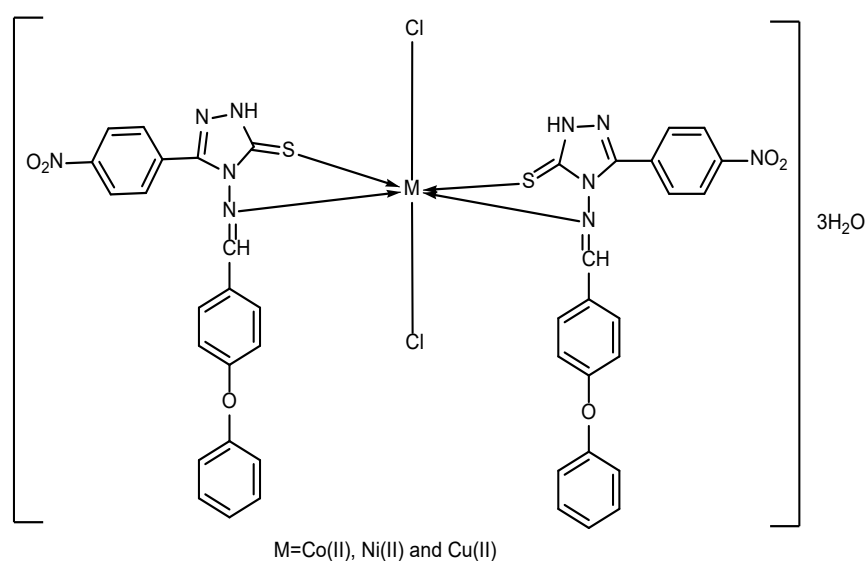


Fig 3. Suggestion of metal complexes

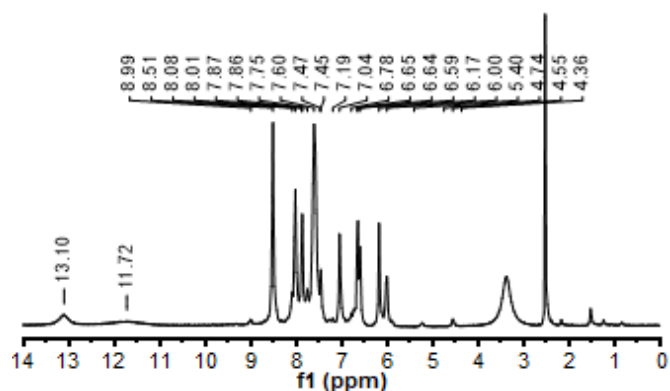


Fig 4. ^1H -NMR spectrum of Schiff base (Ligand L)

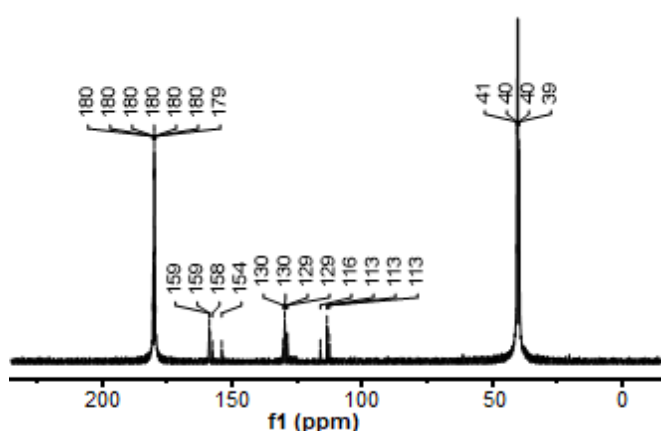


Fig 5. ^{13}C -NMR Spectrum of Schiff base (Ligand L)

chemically between 112 ppm and 130 ppm [17].

Thermal Analysis

Thermogravimetric analysis

Fig. 6 and 7 show indicative TG and DTG curves for the Schiff base ligand and its complexes of a metal ion [18] under the nitrogen atmosphere at a rate of $20\text{ }^\circ\text{C}/\text{min}$. Table 5 shows the function of the temperature. Overall, the TG curves of the C_1 , C_2 , and C_3 complexes displayed an early loss of weight due to evaporation of moisture, followed by a degradation step up to $200\text{ }^\circ\text{C}$, and an extended degradation up to almost $900\text{ }^\circ\text{C}$ for C_1 and C_2 complexes, and $600\text{ }^\circ\text{C}$ for C_3 complex. The latter decomposition was where the majority of the weight loss occurred, with a final degradation that led to a total weight loss of over 80%. Thus, after the moisture evaporation, the first degradation step of complexes was attributed to the thermal vaporization of volatile compounds. The second degradation step was most probably due to the loss of molecules from the complexes. Similarly, the Schiff base ligand (L) showed two degradation steps after dehydration [19-20]. Furthermore, the DTG curves had a small peak related to moisture loss; a steep top, which maximum temperature values were also recorded in Table 5; as well

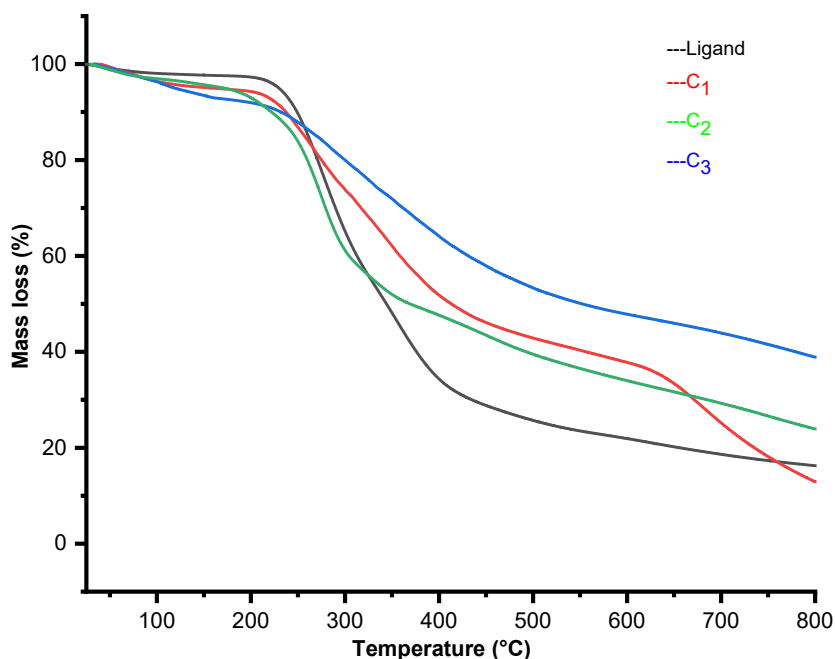


Fig 6. TG curves of the ligand and its metal ion complexes under nitrogen atmosphere at a heating rate of $20\text{ }^\circ\text{C}/\text{min}$

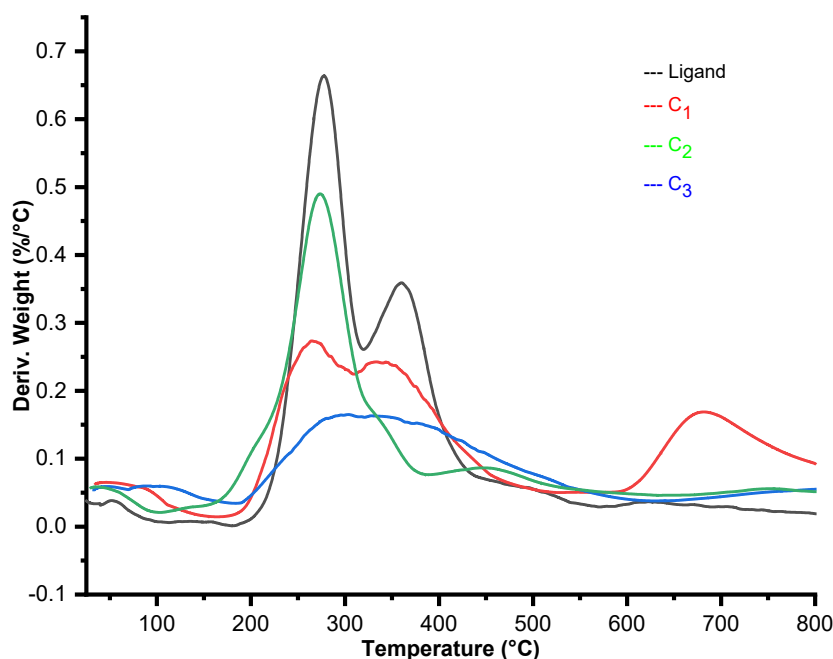


Fig 7. DTG curves of the ligand and its metal ion complexes under nitrogen atmosphere at a heating rate of 20 °C/min

Table 5. Thermal decomposition data of TG/DTG curves for the ligand and its metal ion complexes under nitrogen atmosphere

Compound	Molecular formula	Molecular weight (g/mol)	Step	Temperature range of the decomposition (°C)	Mass (%)	DTG maxima (°C)
Ligand L	$C_{21}H_{15}O_3N_5S$	417	1	0–175	2.469	
			2	175–340	40.63	275
			3	340–560	33.59	362
			4	560–1000	12.55	
			5	> 1000	10.761	
C ₁	$[Co(L)_2Cl_2] \cdot 2H_2O$	1072	1	0–160	7.556	
			2	160–620	45.08	290
			3	620–1000	19.89	
			4	> 1000	27.474	
C ₂	$[Ni(L)_2Cl_2] \cdot 2H_2O$	998.73	1	0–95	3.071	
			2	95–390	48.33	
			3	390–635	16.06	273
			4	635–1000	17.32	
			5	> 1000	15.219	
C ₃	$[Cu(L)_2Cl_2] \cdot 2H_2O$	988.73	1	0–180	4.997	
			2	180–360	23.12	267
			3	360–540	30.68	339
			4	540–1000	38.47	677
			5	> 1000	2.733	

as a slight minimum owing to moisture loss, except for C1 that had a large and broad peak located between 600–900 °C. More interestingly, all of the complexes had

virtually the same breakdown temperature, which was in the range of 180 °C to 400 °C, indicating that they were thermally stable. The temperature at which degradation

began has been suggested to confirm the comparative stability of the complexes. Unlike C₃ complex, C₁ and C₂ degradation continued at temperatures higher than 600 °C [20-21].

■ CONCLUSION

Based on the process described in the literature, 2-amino-triazole derivative and 4-phenoxybenzaldehyde produced the Schiff bases (ligand L). The new ligands exhibited bidentate behavior in all metal complexes, with at least one of the nitrogen of azomethine and thiol groups being used as a chelate to coordinate with copper(II), nickel(II), and cobalt(II) metal ions. The complexes were synthesized with the new ligand according to 1:2 molar ratio of the complexes and were characterized using FTIR, ¹³C-NMR, and ¹H-NMR to confirm the structures. Other analyses, such as magnetic property measurements, molar conductance, elemental analysis (CHNS), thermal analysis (TG, DTG), and atomic absorption were also performed. The results indicated that the complexes' proposed structures had an octahedral geometry. Thermogravimetric analyses of metal complexes were carried out in an inert atmosphere from room temperature to 1000 °C at 20 °C/min of heating rate. We were able to investigate their thermal deterioration profile using TGA/DTG. Thus, the degradation of the major components occurred in two steps for C₁ and C₂ complexes, and one step for C₃ complexes. These results could be used to predict the study biology activities behavior of these complex and could help in the evaluation of the could become a basis for further studies and at in-vitro and in-vivo levels experimental and this excellent performance would encourage us to develop more triazole derivative.

■ REFERENCES

- [1] Al-Khazraji, A.M.A., and Al Hassani, R.A.M., 2020, Synthesis, characterization and spectroscopic study of new metal complexes form heterocyclic compounds for photostability study, *Sys Rev Pharm.*, 11 (5), 535–555.
- [2] Sumrra, S.H., Sahrish, I., Raza, M.A., Ahmad, Z., Zafar, M.N., Chohan, Z.H., Khalid, M., and Ahmed, S., 2020, Efficient synthesis, characterization, and in vitro bactericidal studies of unsymmetrically substituted triazole-derived Schiff base ligand and its transition metal complexes, *Monatsh. Chem.*, 151 (4), 549–557.
- [3] Bennion, J.C., McBain, A., Son, S.F., and Matzger, A.J., 2015, Design and synthesis of a series of nitrogen-rich energetic cocrystals of 5,5'-dinitro-2H,2H'-3,3'-bi-1,2,4-triazole (DNBT), *Cryst. Growth Des.*, 15 (5), 2545–2549.
- [4] Peng, Z., Wang, G., Zeng, Q.H., Li, Y., Wu, Y., Liu, H., Wang, J.J., and Zhao, Y., 2021, Synthesis, antioxidant and anti-tyrosinase activity of 1,2,4-triazole hydrazones as antibrowning agents, *Food Chem.*, 341, 128265.
- [5] Mentese, E., Akyüz, G., Emirik, M., and Baltaş, N., 2019, Synthesis, *in vitro* urease inhibition and molecular docking studies of some novel quinazolin-4(3H)-one derivatives containing triazole, thiadiazole and thiosemicarbazide functionalities, *Bioorg. Chem.*, 83, 289–296.
- [6] Dalloul, H.M., El-nwairy, K., Shorafa, A.Z., and Samaha, A.A., 2017, Synthesis and biological activities of some new spiro 1,2,4-triazole derivatives having sulfonamide moiety, *Org. Commun.*, 10 (4), 280–287.
- [7] Jin, R., Wang, Y., Guo, H., Long, X., Li, J., Yue, S., Zhang, S., Zhang, G., Meng, Q., Wang, C., Yan, H., Tang, Y., and Zhou, S., 2020, Design, synthesis, biological activity, crystal structure and theoretical calculations of novel 1,2,4-triazole derivatives, *J. Mol. Struct.*, 1202, 127234.
- [8] Sahoo, P.K., Sharma, R., and Pattanayak, P., 2010, Synthesis and evaluation of 4-amino-5-phenyl-4H-[1,2,4]-triazole-3-thiol derivatives as antimicrobial agents, *Med. Chem. Res.*, 19 (2), 127–135.
- [9] Bader, A.T., Rasheed, N.A., Aljeboree, M., and Alkaiml, A.F., 2020, Synthesis, characterization of new 5-(4-nitrophenyl)-4-((4 phenoxybenzylidene) amino)-4H-1,2,4-triazole-3-thiol metal complexes and study of the antibacterial activity, *J. Phys. Conf. Ser.*, 1664, 012100.

- [10] Emam, S.M., Tolan, D.A., and El-Nahas, A.M., 2020, Synthesis, structural, spectroscopic, and thermal studies of some transition-metal complexes of a ligand containing the amino mercapto triazole moiety, *Appl. Organomet. Chem.*, 34 (5), e5591.
- [11] Venugopala, K.N., Kandeel, M., Pillay, M., Deb, P.K., Abdallah, H.H., Mahomoodally, M.F., and Chopra, D., 2020, Anti-tubercular properties of 4-amino-5-(4-fluoro-3-phenoxyphenyl)-4*H*-1,2,4-triazole-3-thiol and its Schiff bases: Computational input and molecular dynamics, *Antibiotics*, 9 (9), 559.
- [12] Rapheal, P., Manoj, E., Kurup, M.R.P., and Fun, H.K., 2021, Nickel(II) complexes of N(4)-substituted thiosemicarbazones derived from pyridine-2-carbaldehyde: Crystal structures, spectral aspects and Hirshfeld surface analysis, *J. Mol. Struct.*, 1237, 130362.
- [13] Hamil, A., Khalifa, K.M., Almutaleb, A.A., and Nouradean, M.Q., 2020, Synthesis, characterization and antibacterial activity studies of some transition metal chelates of Mn(II), Ni(II) and Cu(II) with Schiff base derived from diacetylmonoxime with O-phenylenediamine, *Adv. J. Chem. A*, 3 (4), 524–533.
- [14] Kargar, H., Torabi, V., Akbari, A., Behjatmanesh-Ardakani, R., Sahraei, A., and Tahir, M.N., 2020, Pd(II) and Ni(II) complexes containing an asymmetric Schiff base ligand: Synthesis, X-ray crystal structure, spectroscopic investigations and computational studies, *J. Mol. Struct.*, 1205, 127642.
- [15] Mahmoud, N.F., Abbas, A.A., and Mohamed, G.G., 2021, Synthesis, characterization, antimicrobial, and MOE evaluation of nano 1,2,4-triazole-based Schiff base ligand with some d-block metal ions, *Appl. Organomet. Chem.*, 35 (6), e6219.
- [16] Silverstein, R., Webster, F.X., and Kiemle, D., 2005, *Spectrometric Identification of Organic Compounds*, 7th Ed., John Wiley & Sons, Inc., Hoboken, New Jersey, USA.
- [17] Amer, S., El-Wakiel, N., and El-Ghamry, H., 2013, Synthesis, spectral, antitumor and antimicrobial studies on Cu(II) complexes of purine and triazole Schiff base derivatives, *J. Mol. Struct.*, 1049, 326–335.
- [18] Magyarai, J., Holló, B.B., Rodić, M.V., Jovanović, L.S., Szécsényi, K.M., Ferenc, W., Osypiuk, D., Mosolygó, T., Kincses, A., and Spengler, G., 2020, Synthesis, characterization, thermal properties and biological activity of diazine-ring containing hydrazones and their metal complexes, *J. Therm. Anal. Calorim.*, 2020, 1–14.
- [19] Abid, M.N., Hafith, F.R., Musa, T.M., and Abbas, B.F., 2021, Synthesis, characterization and biological activity study of cobalt(II), nickel(II) and copper(II) complexes derived from mixed bidentate ligands of oxime and phenanthroline, *Egypt. J. Chem.*, 64 (11), 6487–6492.
- [20] Chaurasia, M., Tomar, D., and Chandra, S., 2019, Synthesis, spectral characterization, and DNA binding studies of Co(II), Ni(II), Cu(II) and Zn(II) complexes of Schiff base 2-((1*H*-1,2,4-triazol-3-ylimino)methyl)-5-methoxyphenol, *J. Mol. Struct.*, 1179, 431–442.
- [21] Gaber, M., El-Ghamry, H.A., and Fathalla, S.K., 2020, Synthesis, structural identification, DNA interaction and biological studies of divalent Mn, Co and Ni chelates of 3-amino-5-mercapto-1,2,4-triazole azo ligand, *Appl. Organomet. Chem.*, 34 (8), e5678.